GTP-21-1313

A Study on Fundamental Combustion Properties of Oxymethylene Ether-2

John M. Ngugi*, Sandra Richter, Marina Braun-Unkhoff,

Clemens Naumann, Markus Köhler, Uwe Riedel[1]

German Aerospace Center (DLR)

Institute of Combustion Technology

Pfaffenwaldring 38-40, 70569 Stuttgart, Germany

[1] German Aerospace Center (DLR)

Institute of Low-Carbon Industrial Processes

Walther-Pauer-Straße 5, 03046 Cottbus, Germany

*Email: john.mburu@dlr.de

ABSTRACT

Oxymethylene ethers (OME_n, n=1-5) are a promising class of synthetic fuels that have the potential to be used as additives or substitutes to diesel in compression ignition engines. A comprehensive understanding of their combustion properties is required for their safe and efficient utilization. In this study, the results of a combined experimental and modeling work on oxidation of OME_2 are reported: (i) Ignition delay time measurements of stoichiometric OME_2 / synthetic air mixtures diluted 1:5 with nitrogen using the shock tube method at pressures of 1, 4, and 16 bar, and (ii) laminar flame speeds of OME_2 / air mixtures using the cone angle method at atmospheric and elevated pressures of 3 and 6 bar. The experimental data sets obtained have been used for validation of three detailed reaction mechanisms of OME_2 obtained from literature. The results of ignition delay time measurements showed that ignition of OME_2 is characterized by pre-ignition activity at the low temperature side of the measurements regardless of the pressure. Regarding the performance of the different reaction mechanisms, the model from Cai *et al.* (2020) best predicted the temperature and pressure dependence of ignition delay times. For laminar flame speeds, the experimental data were well matched by the mechanism from Ren *et al.* (2019) at p = 1, 3, and 6 bar and for all equivalence ratios considered.

From sensitivity analyses calculations, it was observed that chain reactions involving small radicals, *i.e.*, H, O, OH, HO_2, and CH_3 control the oxidation of OME_2. The comparison of the results of this work and our previous work (Ngugi et al. (2021)) on OME_1 show that these two fuels have similar oxidation pathways. The results obtained in this work will contribute to a better understanding of the combustion of oxymethylene ethers, and thus, to the design and optimization of burners and engines as well.

Keywords: Oxymethylene ether, synthetic fuels, laminar flame speed, ignition delay time, reaction mechanism.

INTRODUCTION

Diesel engines widely used in ground transportation and haulage are heavily reliant on fossil fuels. The decarbonization of this sector is of crucial importance to reduce climate effects, while emissions of soot particles and NO_x are harmful to the environment and human health [1]. In the wake on improving the local air quality in cities and on fostering the use of renewable sources, alternative fuels offer the chance on addressing both points [2, 3]. This becomes apparent for different time scales, where a wide range of different approaches are needed for future transportation systems. In addition to electric solutions, hydrogen-based strategies are a welcome addition to this mix enabling CO_2 emission free transportation. However, in addition to technological challenges such as motors and propulsion concepts, a new infrastructure for energy distribution is essential. While in the long term these concepts are highly promising, alternative fuels offer a solution with the use of already existing infrastructure and vehicles with little to none adjustments but contributing to CO_2 neutral emissions. The requirement of diesel engines to meet stringent emission regulation requirements such as Euro VI [4] are already high, but may become even more stringent with the currently discussed Euro VII. As a result, there has been a major focus towards reduction of emissions in the transport sector through the deployment of low-emission advanced alternative fuels, such as alcohols and renewable synthetic fuels [2-3, 5].

Oxymethylene ethers (OME_n) are a recent class of synthetic alternative fuels with the molecular formula of $CH_3O(CH_2O)_nCH_3$ (with $n \geq 1$). OME_n have been promoted because of their ability to burn in diesel engines with reduced emissions of soot and nitrogen oxides (NO_x) compared to diesel fuel [6-12]. OME_n has the potential to be employed immediately as drop-in fuels since they can be used in diesel engines with almost no modification; their

deployment can also benefit through the existing distribution infrastructure [10-11]. OME_n can be produced from renewable sources at a large scale in two prominent ways: (i) by power-to liquid technology (PtL) using renewable sources: wind or solar power and CO_2 removal from air [10,12]; (ii) via biomass routes through gasification or fermentation of sugars [13,14]. In future, ethers might play a role as an alternative fuel (blend) for power generation in gas turbines. OME_n have further attractive properties such as higher cetane number, typically above 55, and a better mixing with air due to the fast evaporation rates [15].

To this end, a comprehensive understanding of fundamental combustion properties of OME_n, *e.g.* auto ignition and flame speeds, is a prerequisite for the evaluation of their engine application potential and in the development of safe and more advanced engines and burners. The fundamental combustion properties, *i.e.* auto ignition and laminar burning velocities of OME_1, the smallest oxymethylene ether, have been studied widely in literature as reviewed in our previous work [16]. However, only few studies on auto ignition and flame speeds of OME_{2-4} are available as summarized in Table 1. No data for auto ignition of OME_{2-4} is available for temperatures larger than 1150 K and for pressures of 1 bar. Regarding laminar flame speeds of OME_2 / air mixtures, the first measurements were recently performed by Eckart *et al*. [17] at p = 1 bar in a temperature range between 383 - 401 K.

The primary objective of this work is to study auto ignition and laminar flame speeds of OME_2 through a combined experimental and modeling approach. The ignition delay times (IDTs) of OME_2 / ($20\%O_2$+$80\%N_2$) diluted 1:5 in N_2 were measured behind the reflected shock wave employing the shock tube method at atmospheric and elevated pressures and covering up to the high temperature range. The laminar burning velocities of OME_2 / air at atmospheric and at elevated pressures have been determined by using a Bunsen type burner and by applying the cone angle method. Moreover, all the measurements in this work are compared to the results of calculations with up to three detailed reaction models taken from literature, see Table 2.

EXPERIMENTAL

To study the combustion properties of OME_2, ignition delay times and laminar burning velocities were measured. Table 3 gives a summary of the composition of fuel-oxidizer/diluent mixtures studied and pressure and temperature

regime covered.

Measurement of ignition delay times

All the ignition delay time measurements in this work were carried out in a shock tube with an inner diameter of 9.82 cm (see Fig. 1), which has been described in previous studies [22-30]. Herein, only a brief introduction of this apparatus is provided.

The shock tube is operated with a double aluminum diaphragm arrangement introducing a small intermediate section that separates the 5.88 m long driver section and the 11.348 m long driven section. The driven section is heated to 373 K to prevent condensation of the fuel. Prior to initiating the shock wave, the driver and driven sections are evacuated to pressures at least below 5.0×10^{-6} mbar by a turbomolecular pump. The driven section is then filled with the test mixtures while the driver and intermediate sections are filled either with helium or with the tailored helium / argon mixtures. Two Bronkhorst mass flow system controlled the gas flows to achieve tailored interface and thus, extend the observation period. Both helium and argon have a purity of above 99.996%.

The measurement section of the shock tube has four pressure transducers (type PCB 113B24) flush mounted on the side wall (see Fig. 1). They are connected to the counters (type HAMEG HM 8123) which record the time for the arrival of the incident and reflected shock wave. The incident (u_1) and the reflected velocity (u_5) of the shock wave are calculated from the recorded time intervals and the constant distance of 200 mm between the pressure transducers. The speed of the incident shock wave at the end flange is determined by linear extrapolation of the axial velocity profile to the end wall. The temperature and pressure behind the reflected shock wave were calculated from a one-dimensional normal shock model with measured incident shock velocity and velocity attenuation, initial temperature, and pressure as well as the fuel/oxidizer/diluent mixture composition as input parameters. The thermodynamic data for OME_2 was obtained from Cai *et al.* [14]. The estimated uncertainty in the initial reflected shock temperature is less than ±15 K @ 1000 K.

The ignitable mixtures of fuel/oxidizer diluted 1:5 in N_2 were prepared in a stainless-steel vessel heated at a constant temperature of 373 K and evacuated to pressures below 5×10^{-6} mbar. This temperature was high enough to

prevent any condensation and low enough to reduce thermal degradation of the fuel. The fuel was injected to the evacuated tank separately to its respective partial pressure corresponding to molar composition specified in Table 3. Synthetic air (the oxidizer) was then charged to achieve the desired equivalence ratio upon controlling the pressure and the amount of the injected fuel. Finally, the fuel/synthetic air mixture was diluted with N_2 (20% fuel-oxidizer mixture: 80% N_2, defined as dilution ratio of 1:5). The mixture was left to settle at least 24 hours before the experiments to ensure a good mixing. The gases used were obtained from Linde with the following purities: O_2 - 99.9999%, N_2 - 99.9999%, and synthetic air - 99.999%. OME_2 was obtained from Analytik-Service GmbH (ASG) with a purity of 98.81%-mass with the remaining part mainly OME_1. The degradation of the fuel/oxidizer/diluent mixture and the residual compounds was checked and monitored by gas chromatographic tests. Thermo decomposition products OME_1 and methanol were detected and their levels continuously monitored. The mixture had to be consumed within two days so that the average combined levels of OME_1 and methanol relative to OME_2 are kept within the range of 5%.

Figure 2 shows an example of a pressure profile and normalized emission signal (linearized) from a single experiment undertaken at p_{init} = 14.4 bar and T_{init} = 868 K for determination of ignition delay time. In this work, all ignition delay time values are derived from the time difference between the instance of formation of reflected shock wave at the endplate (t/s = 0) and the occurrence of maximum emission of CH* observed through the radial port (measurement plane) and alternatively through the axial port (endplate), see Fig. 2. The pressure behind the reflected shock wave is observed to increase in two steps. In the first step, a gradual increase in pressure ends up at about 7000 µs due to gas dynamics caused by the interaction of the reflected shock wave with the boundary layer formed behind the reflected shock wave. For the conditions of this shock, this increase in pressure is more pronounced because of the extended observation period. The second increase in pressure, from about 7000 µs to about 9500 µs, is attributed to heat release and ignition. The emission signal remains at zero level up to about 7900 µs followed by a steep rise indicating the onset of ignition activity. The emission signal shows a clear two step-ignition process with the main ignition at about 12300 µs and pre-ignition at about 8200 µs. We observe that the onset of pre-ignition activity corresponds to the onset of heat release. In this case, ignition delay times are derived from the main peak. Also, the time of occurrence of maxima of the pre-ignition peak is derived.

Measurement of laminar burning velocity

The measurements were performed at a preheat temperature of T = 473 K and pressures of p = 1 bar, 3 bar, and 6 bar. At 1 bar, the covered range of equivalence ratio (φ) lies between φ = 0.6 and φ = 2.0. Since the used experimental setup as well as the determination of the laminar burning velocity were already described in our previous studies [16, 24, 27], where more detailed information of the experiment is given, here the experiment is concisely described:

The fuel OME_2 (ASG Analytik-Service Gesellschaft, 98.81% - mass) was vaporized at 413 K (140 °C) at 1 bar using an HPLC-pump (type LC-20AD, Shimadzu) to control the flow rate. At elevated pressures, the vaporization temperature was adjusted to 443 K (170 °C, 3 bar) and 493 K (220 °C, 6 bar), respectively. After vaporization, OME_2 was mixed with a preheated nitrogen stream (N_2, Linde, 99.999%). This mixture was adjusted to the preheat temperature of 473 K, and preheated oxygen (O_2, Linde, 99.95%) was added so that the ratio between nitrogen and oxygen is in accordance with the composition of air (N_2:O_2 = 79:21). The flow rates of N_2 and O_2 were controlled by calibrated mass flow controllers (Bronkhorst, type F-111B). The time of contact with O_2 at preheat temperature in the fuel preparation line is limited to less than 0.5 s @ 1 bar and 5 s @ 6 bar.

Premixed conical-shaped flames have been stabilized using flame holders with contracting nozzles of different diameters depending on the pressure during measurement. The use of a coflow enables the flame stabilization over a wide φ-range. The composition of the used coflow was the same as reported in previous publications, *e.g.* [16, 27] – air for fuel rich flames, and a mixture of 5% CH_4 + 5% H_2 + 90% N_2 for fuel lean flames.

The determination of the laminar burning velocity S_u is based on the cone angle method [16, 24]. For the cone angle detection, pictures of the flames were recorded with a CCD-camera (type Imager Intense, LaVision). From the visible cone angle α and the velocity v_u of the unburned gas, S_u values were calculated according to equation (1):

$$S_u = v_u \cdot \sin\alpha \qquad \text{(Eq. 1).}$$

The experimental uncertainty for the determination of the burning velocities depends on the pressure and the fuel-air ratio. At 1 bar, the uncertainty amounts to ±2-5%, with about ±6% for very fuel rich mixtures ($\varphi \geq 1.9$) and up to ±9% for very fuel lean mixture ($\varphi < 0.8$). At elevated pressures, the uncertainties are between ±2% and ±9%, with up to ±13% for fuel rich mixtures ($\varphi > 1.4$). The uncertainties are attributed to difficulties in flame stabilization resulting

to varying cone angles. In addition, pressure fluctuations and the accuracies of the mass flow controllers also contribute to the uncertainties. For a more detailed discussion, see Refs. [23-25, 27].

MODELING

Laminar flame speeds calculations were performed by using the open-source software Cantera [32] assuming a freely propagating flame and employing the multi-component diffusion model and thermo-diffusion. Ignition delay calculations are based on the 0-dimensional homogeneous reactor model as implemented within the SENKIN Code [33]. In addition, an experimentally derived pressure profile $p = p(t)$ was incorporated into the modeling calculations to account for the post-shock compression pressure rise due gas dynamic effects only, not regarding any pressure rise due to heat release; for more details, see [16, 22, 27].

RESULTS AND DISCUSSION

The comparison between measured and predicted data is discussed. First, ignition delay times determined for p / bar = 1, 4, and 16 for OME_2 (Figs. 3 and 4) are presented, with the reaction models used given in Table 2. Results for ignition delay sensitivities for OME_2 using the mechanism given by Cai *et al.* [14] are provided in Fig. 5. Secondly, the comparison between measured and calculated laminar burning of OME_2 / air mixtures are discussed for p / bar = 1, 3, and 6 (Figs. 6-7) using the models from Cai *et al.* [14], Sun *et al*. [20], and Ren *et al.* [21].

Measurement of ignition delay times

In Fig. 3, ignition delay times (radial and axial) are plotted versus inverse temperature for a stoichiometric mixture of OME_2 / synthetic air at a dilution of 1:5 (20% mixture / 80% N_2) at initial pressures of 1, 4, and 16 bar. It is observed that the axially and radially derived ignition delay times of the 16 bar series fail to converge in the high temperature regime, typically above 1400 K. This is attributed to the different speeds of the reflected shock wave and the combustion wave [31]. The detection setup comparison of both emission signals (radial and axial) allows reducing the uncertainty of ignition delay time measurements at the highest temperatures to ±30% although the blast wave correction is needed for the radial port emission detection measurements, especially for short ignition delay times. The axially measured emission is determined by the dynamic of the propagation of the deflagration initiated after the ignition. At our experimental conditions, blast wave correction can be up to about 20 µs. Nevertheless, for very short

ignition delay times, typically around and below 20 μs, the axially measured emission signal is taken as upper bound, because for axial emission detection there is no need for blast wave correction.

At elevated pressures (4 and 16 bar), we observe a non-linear behavior of ignition delay times becoming shorter for temperatures lower than about 1100 K mainly due to the rise in temperature due to post shock compression process. Ignition delay times were measured up to 12500 μs, depending on temperature and pressure as outlined in Fig. 3. Also, it is depicted that the trend of ignition delay times is decreasing with increasing pressure for all the temperatures due to increased reactivity of the system.

The comparison between measured (symbols) and the results of calculations (curves) Chemkin II package and reaction models from Cai *et al.* [14], Sun *et al*. [20], and Ren *et al.* [21] are presented in Fig. 4. For long ignition delay times, a pressure profile derived from shocks with long ignition delay times and those from non-ignitable synthetic air mixtures had to be applied to account for the pressure rise caused by gas dynamics effects. The measured ignition delay times are generally matched by predicted data from the three reaction models. However, at 1 bar we observe that the model from Sun *et al.* [20] slightly overpredicts the ignition delay times especially for temperatures above 1250 K. The mechanism from Cai *et al.* [14] best reproduced the non-linear dependency of ignition delay time data becoming shorter with decreasing temperature. In the low temperature regime, starting from 1000 K at 4 bar and 1250 K at 16 bar, the three models fail to converge. It should be noted that the Sun *et al.* [20] model was designed for high-temperature oxidation of OME_3 but also includes the oxidation pathways for OME_1 and OME_2. On the other hand, the Ren *et al.* [21] model was designed for high and low temperature oxidation of primary reference fuels and OME_2. These two models [20, 21] were not validated against experimental data for OME_2.

In this work, it is shown that ignition of stoichiometric mixtures of OME_2 / synthetic air at a dilution of 1:5 with nitrogen is characterized by pre-ignition activity at the low temperature side of the measurements. In Fig. 4, the time of occurrence of maxima of the pre-ignition peaks (see the 'stars') is compared to the main ignition and the results of calculation using the three models. It is observed that the model from Cai *et al.* [14] also reproduces the pre-ignition activity, see the red-dashed curve in Fig. 4. In Fig. 5, a comparison is made to the measured ignition delay times of stoichiometric OME_1 / synthetic air mixtures [16] at p / bar = 1 and 16. It is observed that ignition delay times of OME_2 are shorter than those of OME_1, particularly for temperatures lower than 1450 K.

Sensitivity analysis

The sensitivity analyses of ignition delay times have been performed with respect to the rate coefficient of each reaction at constant pressures of 1, 4, and 16 bar. For each pressure, the sensitivity calculations were performed at three temperatures, 1000 K, 1300 K, and 1600 K, using the mechanism from Cai *et al.* [14]. Figure 6 shows the normalized sensitivity coefficients (S_i) for stoichiometric OME_2 / synthetic air mixtures at a dilution of 1:5 with N_2. The normalized sensitivity coefficient is defined as: $S_i = (k_i^{ref} / \tau_i^{ref}) * [d\tau_{ign}/dk_i]$, where the superscript 'ref' refers to the unperturbed system. For each pressure, the 15 most important reactions with the highest normalized sensitivities, usually sorted at 1300 K, are presented. The results show that chain reactions involving H, O, OH, HO_2, and CH_3 radicals largely control the ignition process of OME_2. Like many hydrocarbon fuels, the ignition of OME_2 is very sensitive to $H+O_2 \Leftrightarrow O+OH$. Ignition of OME_2 is also very sensitive to the chain branching reaction $CH_3+HO_2 \Leftrightarrow CH_3O+OH$. At the condition considered in this work, it is observed that OME_2 ignition is sensitive to fuel-specific reactions: OME_2 (+ M) $\Leftrightarrow$ $CH_3 + CH_3OCH_2OCH_2O$ (+ M) and OME_2 (+ M) $\Leftrightarrow$ $CH_3OCH_2O + CH_3OCH_2$ (+M). Previously [16], we analyzed the sensitivity analysis of OME_1 at similar conditions of pressure, temperature, and dilution. The conclusion is that the dominant reactions during ignition of OME_2 are very consistent to those of OME_1. This is also in agreement to the findings of Cai *et al.* [14].

Measurement of laminar burning velocities: OME_2

The results of the experimentally determined laminar burning velocities of OME_2 are displayed in Fig. 7. For comparison, values of the laminar flame speed were calculated using the mechanisms from Cai *et al.* [14], Sun *et al*. [20], and Ren *et al.* [21]. The peak values of the measured burning velocities are 105, 84 and 68 cm s^{-1} at 1, 3 and 6 bar, respectively. For the three pressures, the peak values are located at about φ = 1.15-1.20.

According to the calculations shown in Fig. 7, the mechanism from Ren *et al.* [21] offers the best predictability of the laminar flame speed of OME_2, with only a slight overprediction of about 5 cm s^{-1} at p = 1 bar and φ = 1.20 (corresponds to a deviation of < 5%) of the experimental data. At the fuel lean and fuel rich side and as well as at elevated pressures, the deviation is even smaller if ignoring φ-values ≥ 1.7 (at 3 bar) and φ-values ≥ 1.5 (at 6 bar).

Here, the observed underprediction results from a more difficult flame stabilization during the measurement resulting in higher experimental uncertainties, with up to ±13% (see exp. section). In contrast to the results obtained with the mechanism from Ren *et al.* [21], the calculations using the models from Cai *et al.* [14] and Sun *et al*. [20] are underpredicting the φ-values by about 8% for the φ-values > 0.9 at p = 1 bar and p = 3 bar; both models are showing nearly identical modeling results. For smaller φ-values as well as at p = 6 bar up to φ = 1.40 the deviations are distinctly smaller than the experimental uncertainties (see Fig. 7). In these regimes, the models from Cai *et al.* [14] and from Sun *et al*. [20] match quite well with the experimental data.

In Fig. 8, a comparison to the laminar burning velocities of other fuels for p = 1 bar is shown. For OME_1 [14], nearly identical results were obtained caused by the similar structure of the fuels differing merely in an additional -O-CH_2 group of OME_2 compared to OME_1. The comparison to *n*-butanol [24] and PRF90 (primary reference fuel 90 = 90 vol-% *iso*-octane + 10 vol-% *n*-heptane) [23] shows not only distinct higher laminar burning velocities for OME_2 at φ-values > 0.9 but also a different location of the peak, at about φ = 1.10 for *n*-butanol and PRF90. The peak value for the laminar burning velocity of *n*-butanol, belonging to the groups of oxygenated fuels as well, amounts to S_u = 90 cm s^{-1} whereas the one of PRF90, being a reference and surrogate fuel for gasoline, is at about S_u = 80 cm s^{-1}.

Sensitivity analysis

Sensitivity analyses of the OME_2 laminar flame speeds were done using the reaction models from Cai *et al.* [14] and Ren *et al*. [21] for two conditions: (i) at p = 1 bar for φ-values of 0.6, 1.2, and 1.7; and (ii) for φ = 1.2 at p = 1, 3, and 6 bar. The results are given in Fig. 9 displaying the 15 most important reactions for OME_2 combustion. These results show that the chain branching reaction ($H + O_2 \Leftrightarrow O + OH$) and reactions with CO involved ($HCO + M \Leftrightarrow CO + H + M$, $H + HCO \Leftrightarrow CO + H_2$, and $CO + OH \Leftrightarrow CO_2 + H$) are the most dominant ones within OME_2 oxidation. It is observed that the variation in φ has almost a greater impact on the reactions than the variation in pressure; see for instance, the reactions $CO + OH \Leftrightarrow CO_2 + H$ and $H + O_2 (+ M) \Leftrightarrow HO_2 (+ M)$. Regardless of the specific model used, it is found that reactions involving smaller radicals have a large influence on the oxidation of OME_2. The results of flame speed measurements show major similarities between the reaction pathways controlling the oxidation of OME_2 observed in this work and of OME_1 as well as observed in our previous work [16].

SUMMARY AND CONCLUSIONS

In the current study, a combined experimental and modeling approach was utilized to study two combustion properties, *i.e*., ignition delay times and laminar flame speeds of OME_2. Ignition delay times of stoichiometric mixtures of OME_2 / synthetic air at a dilution of 1:5 (20% mixture / 80% N_2) were measured in a shock tube at pressures p = 1, 4, and 16 bar while burning velocities of OME_2/air mixtures were determined at pressures p = 1, 3, and 6 bar and at a pre-heat temperature of T = 473 K for equivalence ratios φ between $0.6 \leq \varphi \leq 1.8$ using a Bunsen type burner and employing the cone angle method. A comparison was presented between experimental and calculated data using three chemical kinetic reaction models from literature.

The ignition delay time data decreased with increasing pressure; the non-linear dependency of ignition delay times with reducing temperature was mainly attributed to gas dynamics effects. Overall, there was a good agreement between the experimental data and the prediction with the models, with some room for improvement for the models of Sun *et al*. [20] and Ren *et al.* [21] in the high-temperature region. The ignition delay time data showed that in the low-temperature regime, typically below 1250 K, a two-step ignition process was observed. The model from Cai *et al.* [14] captures well the temperature and pressure dependency of ignition delay times; thus, the Cai *et al.* [14] model confirms the two step-ignition behavior observed in the experiments.

The comparison between the laminar burning velocity measurement showed that predictions made using the model of Ren *et al.* [21] had the best agreement with measurements at p = 1, 3 and 6 bar for all equivalence ratios considered. The results of the sensitivity analysis of ignition and of flame speed revealed that reactions involving small radicals, *i.e.*, H, O, OH, HO_2, and CH_3, largely control the ignition of OME_2. For flame speeds, it is observed that the variation in equivalence ratio has a larger impact on specific reactions than the variation in pressure. The comparison of the results of this work on OME_2 and those of our previous work [16] on OME_1 reveals similar oxidations pathways between these two important oxygenated fuels.

This study is part of our ongoing work on the systematic investigation of combustion properties of ethers including the effect of chain length. The results obtained in this work will form an experimental data base for validation and optimization of chemical kinetic reaction models of OME_2.

Acknowledgments

We thank N. Ackermann for his help in the experimental setup. J.M.N. gratefully acknowledges the financial support by National Research Fund of Kenya and DAAD (Funding programme No: 57399475).

Nomenclature

p	Pressure
t	Time
S_u	Laminar flame speed
S_i	Sensitivity coefficient
v	Velocity of gas mixture

Greek letters

α	Cone angle
λ	Wavelength
φ	Fuel equivalence ratio
τ	Ignition delay time

Subscripts

5	Status behind reflected shock wave
0	initial
l	laminar
ign	Ignition
u	unburnt

References

[1] Fujishima, H., Satake, Y., Okada, N., Kawashima, S., Matsumoto, K., Saito, H., 2013: "*Effects of diesel exhaust particles on primary cultured healthy human conjunctival epithelium*", Ann. of Allergy, Asthma and Immunol. 110(1), 39-43.

[2] Emberger, G., 2017: "*Low carbon transport strategy in Europe: A critical review*", Int. J. of Sustain. Trans 11(1), 31-35.

[3] European Commission, 2016: *"Communication from the commission to the European parliament, the council, the European economic and social committee and the committee of the regions: A European strategy for low-emission mobility"*, Commission Staff Working Document, 244, Accessed 2021-03-16, https://ec.europa.eu/transport/sites/transport/files/themes/strategies/news/doc/2016-07-20-decarbonisation/swd %282016%29244.pdf

[4] Kodjak, D., 2015: "*Policies to reduce fuel consumption, air pollution, and carbon emissions from vehicles in G20 nations*", The International Council on Clean Transportation, Accessed 2021-03-16, https://theicct.org/publications/policies-reduce-fuel-consumption-air-pollution-and-carbon-emissions-vehicles-g20

[5] U.S. Energy Information Administration, 2019: *"International Energy Outlook 2019 with projections to 2050",* U.S. Department of Energy, Accessed 2021-03-16, https://www.eia.gov/outlooks/ieo/

[6] Liu, H., Wang, Z., Li, Y., Zheng, Y., He T., Wang, J., 2019: *"Recent progress in the application in compression ignition engines and the synthesis technologies of polyoxymethylene dimethyl ethers*", Appl. Energy 233, 599-611.

[7] Omari, A., Heuser, B., Pischinger, S., 2017: *"Potential of oxymethylene ether-diesel blends for ultra-low emission engines"*, Fuel 209(1), 232-237.

[8] Iannuzzi, S. E., Barro, C., Boulouchos, K., Burger, J., 2016: "*Combustion behavior and soot formation/oxidation of oxygenated fuels in a cylindrical constant volume chamber*", Fuel 167, 49-59.

[9] Dworschak, P., Berger, V., Härtl, M., Wachtmeister, G., 2020: "*Neat Oxymethylene Ethers: Combustion Performance and Emissions of OME_2, OME_3, OME_4 and OME_5 in a Single-Cylinder Diesel Engine No. 2020-01-0805*", SAE Tech. Paper.

[10] Deutz, S., Bongartz, D., Heuser B., Kätelhön A., Langenhorst LS, Omari A, Walters M, Klankermayer J, Leitner W, Mitsos A., Pischinger S., 2018: "*Cleaner production of cleaner fuels: wind-to-wheel–environmental assessment of CO_2-based oxymethylene ether as a drop-in fuel"*, *Energy & Env. Sci.* 11(2), 331-43.

[11] Omari, A., Heuser, B., Pischinger, S., Rüdinger, C., 2019: "*Potential of long-chain oxymethylene ether and*

oxymethylene ether-diesel blends for ultra-low emission engines", Appl. Energy 239, 1242-1249.

[12] Burger, J., Siegert, M., Ströfer, E., Hasse, H., 2010: "*Poly (oxymethylene) dimethyl ethers as components of tailored diesel fuel: Properties, synthesis and purification concepts*", Fuel 89(11), 3315-3319.

[13] Schmitz, N., Burger J., Ströfer E., Hasse H., 2016: *"From methanol to the oxygenated diesel fuel poly(oxymethylene) dimethyl ether: An assessment of the production costs"*, Fuel 185, 67-72.

[14] Cai, L., Jacobs, S., Langer, R., vom Lehn, F., Heufer, K. A., Pitsch, H., 2020: "*Auto-ignition of oxymethylene ethers ($OME_{n,n=2-4}$) as promising synthetic e-fuels from renewable electricity: shock tube experiments and automatic mechanism generation*", Fuel 264, 116711.

[15] Lin, Q., Tay, K. L., Zhou, D., Yang, W., 2019: "*Development of a compact and robust Polyoxymethylene Dimethyl Ether 3 reaction mechanism for internal combustion engines*". Energy Conv. and Management 185, 35-43.

[16] Ngugi, J. M., Richter, S., Braun-Unkhoff, M., Naumann, C., Riedel, U, 2020: *"An investigation of fundamental combustion properties of the oxygenated fuels DME and OME_1*", Proc. ASME Turbo Expo 2020, GT2020-14702.

[17] Eckart, S., Cai, L., Fritsche, C., vom Lehn, F., Pitsch, H., Krause, H., 2021: "*Laminar burning velocities, CO and NOx emissions of premixed polyoxymethylene dimethyl ether flames*", Fuel 293, 120321.

[18] Drost, S., Schießl, R., Werler, M., Sommerer, J., Maas, U., 2019: "*Ignition delay times of polyoxymethylene dimethyl ether fuels (OME_2 and OME_3) and air: Measurements in a rapid compression machine*", Fuel 258, 116070.

[19] He, T., Wang, Z., You, X., Liu, H., Wang, Y., Li, X., He, X., 2018: "*A chemical kinetic mechanism for the low-and intermediate-temperature combustion of Polyoxymethylene Dimethyl Ether 3 ($PODE_3$)*", Fuel 212, 223-235.

[20] Sun, W., Wang, G., Li, S., Zhang, R., Yang, B., Yang, J., and others, 2017: *"Speciation and the laminar burning velocities of poly(oxymethylene) dimethyl ether 3 ($POMDME_3$) flames: An experimental and modeling study"*, Proc. Combust. Inst. 36(1), 1269-1278.

[21] Ren, S., Wang, Z., Li, B., Liu, H., Wang, J., 2019: "*Development of a reduced polyoxymethylene dimethyl ethers ($PODE_n$) mechanism for engine applications*", Fuel 238, 208-224.

[22] Naumann, C., Janzer, C., Riedel, U., 2019: *"Ethane/Nitrous Oxide Mixtures as a Green Propellant to Substitute Hydrazine: Validation of Reaction Mechanism"*, 9th Proc. Europ. Comb. Meeting, Lisbon (Portugal), Paper-No.: S5_AII_21.

[23] Herzler, J., Herbst J., Kick, Thomas., Naumann C., Braun-Unkhoff M., Riedel U., 2012: *"Alternative fuels based on biomass: an investigation on combustion properties of product gases",* J. Eng. Gas Turbines Power 135 (3), 031401-031401-9, GTP-12-1382.

[24] Methling, T., Richter, S., Kathrotia, T., Braun-Unkhoff, M., Naumann, C., Riedel, U., 2018: *"An Investigation of Combustion Properties of Butanol and Its Potential for Power Generation"*, J. Eng. Gas Turbines Power 140(9), 091505-091505-10, GTP-18-1014, doi: 10.1115/1.4039731.

[25] Richter S., Braun-Unkhoff M., Herzler J., Methling T., Naumann C., Riedel U., 2019: *"An investigation of combustion properties of a gasoline primary reference fuel surrogate blended with butanol"* Proc. ASME Turbo Expo 2019, GT2019-90911.

[26] Herzler, J., Naumann, C., 2008: "*Shock Tube Study of the Ignition of Lean CO/H_2 Fuel Blends at Intermediate Temperatures and High Pressure",* Comb. Sci. Technol. 180(10) 2015-2028.

[27] Richter, S., Kathrotia, T., Naumann, C., Kick Thomas., Slavinskaya, N., Braun-Unkhoff, M., Riedel, U., 2018: *"Experimental and modeling study of farnesane",* Fuel 215, 22-29.

[28] Dagaut, P., Karsenty, F., Dayma, G., Diévart P., Hadj-Ali, K., Mzé-Ahmed, A., Braun-Unkhoff, M., Herzler J., Kathrotia T., Kick, Thomas., Naumann, C., Riedel U., Thomas, L., 2014: *"Experimental and detailed kinetic model for the oxidation of a Gas to Liquid (GtL) jet fuel"*, Combust. Flame 161, 835-847.

[29] Braun-Unkhoff, M., Dembowski, J., Herzler, J., Karle J., Naumann, C., Riedel, U., 2014: "*Alternative Fuels based on Biomass: An experimental and modeling study of ethanol co-firing to natural gas",* J. Eng. Gas Turbines Power 137(9), 091503-091503-9, GTP-14-1640, doi: 10.1115/1.4029625.

[30] Herzler, J., Naumann, C., 2009: "*Shock-tube study of the ignition of methane/ethane/hydrogen mixtures with hydrogen contents from 0% to 100% at different pressures*", Proc. Comb. Inst. 32, 213-220.

[31] Petersen, E. L., 2009: "Interpreting endwall and sidewall measurements in shock-tube ignition studies," *Combust. Sci. and techn. 181(9)*, 1123-1144.

[32] Goodwin, D. G., Moffat, H. K., Speth R.L., 2016: *"Cantera: An object- oriented software toolkit for chemical*

kinetics, thermodynamics, and transport processes", http://www.cantera.org, Version 2.2.1.

[33] Lutz, A. E., Kee, R. J., Miller, J. A. 1988: "SENKIN*: A FORTRAN program for predicting homogeneous gas phase chemical kinetics with sensitivity analysis (No. SAND-87-8248)*". Sandia National Labs., Livermore, CA (USA).

LIST OF FIGURE CAPTIONS

Fig. 1 Schematic diagram of the shock tube [22, 25]. The measurement plane is located 10 mm from the end flange.

Fig. 2 Example of pressure and emission signals of a typical OME_2 / synthetic air mixture with an extended observation period for: φ = 1.0, p_{init} = 14.4 bar, T_{init} = 868 K, and a dilution of 1:5 with N_2.

Fig. 3 Ignition delay times (τ_{ign}) of OME_2 / synthetic air mixtures diluted 1:5 with N_2 at initial pressures p / bar = 1, 4, and 16.

Fig. 4 Comparison of measured (symbols) and simulated (curves) ignition delay times of stoichiometric OME_2 / synthetic air mixtures diluted 1:5 with N_2 for p / bar = 1, 4, and 16 using $p = p(t)$.

Fig. 5 Comparison of measured ignition delay times (τ_{ign}) of synthetic air mixtures of OME_2 (*p.w.*) and of OME_1 [16], at initial pressures p / bar = 1 and 16, φ = 1.0 and 1:5 diluted with N_2. Only radially measured emission data shown.

Fig. 6 Sensitivity of ignition delay time for a mixture of OME_2 / synthetic air calculated for three different temperatures at p / bar = 1, 4, and 16, φ = 1.0, and a dilution d = 1:5 in N_2. Reaction model used: Cai *et al.* [14].

Fig. 7 Measured laminar burning velocities of OME_2-air mixtures (symbols) and calculated laminar flame speeds (curves). Calculations using reaction models from Cai *et al.* [14], Sun *et al*. [20], and Ren *et al.* [21].

Fig. 8 Comparison of the laminar burning velocities of OME_2-air mixtures to measurements of mixtures of OME_1-air [16], *n*-butanol-air [24], and PRF90-air [25] at p = 1 bar.

Fig. 9 Sensitivity analyses of laminar flame speeds of OME_2-air mixtures as a function of φ at p = 1 bar (left) and of p at φ = 1.2 (right). Reaction models used: Cai *et al.* [14] (top) and Ren *et al*. [21] (bottom).

LIST OF TABLE CAPTIONS

TABLE 1: Overview of measured ignition delay times of $OME_{2\text{-}5}$ / oxidizer mixtures. Method: ST–shock tube device, RCM–rapid compression machine, *–pressure specified in atm, CVCV–constant volume cylindrical vessel.

Mixture	***T* / K**	***p* / bar**	***φ***	**Method**	**Ref.**
Ignition delay times					
OME_2/air	650-1120	10, 20	1.0	ST	[14]
OME_3/air	650-1150	10, 20	0.5-2.0	ST	[14]
OME_4/air	750-1100	10, 20	1.0	ST	[14]
OME_2/air	570-690	3-10	1.0	RCM	[18]
OME_3/air/N_2	734-839	10	1.0	RCM	[18]
OME_3/air	640-865	10, 15	0.5-1.5	RCM	[19]
Flame Speeds					
OME_2/air	383-401	1	0.6-1.9	Heat flux	[17]
OME_3/air	408	1 *	0.7-1.6	CVCV	[20]

TABLE 2: Details of kinetic models used in this work.

Reference	Species	Reactions
Cai *et al.* [14]	325	1639
Sun *et al.* [20]	274	1674
Ren *et al.* [21]	149	696

TABLE 3: Fuel-air mixtures studied in present work (*p.w.).*

Mixture	**Parameter range**		
	Fuel-air ratio φ	p / bar	T / K
A. Ignition delay time; dilution 1:5 with N_2			
Composition given in ppm			
OME_2 / synthetic air (20% O_2 + 80% N_2):	1.0	1	1050-1700
7428 ppm OME_2		4	930-1680
274 ppm OME_1		16	850-1670
133 ppm CH_3OH			
38493 ppm O_2			
953672 ppm N_2			
B. Burning velocity: Preheat temperature T_{preh} = 473 K			
Composition given in molar fraction for φ = 1.0			
OME_2 / air (21% O_2 + 79% N_2):	0.6 – 2.0	1	473
0.0403 OME_2	0.7 – 1.8	3	473
0.2015 O_2	0.7 – 1.7	6	473
0.7582 N_2			

Figures

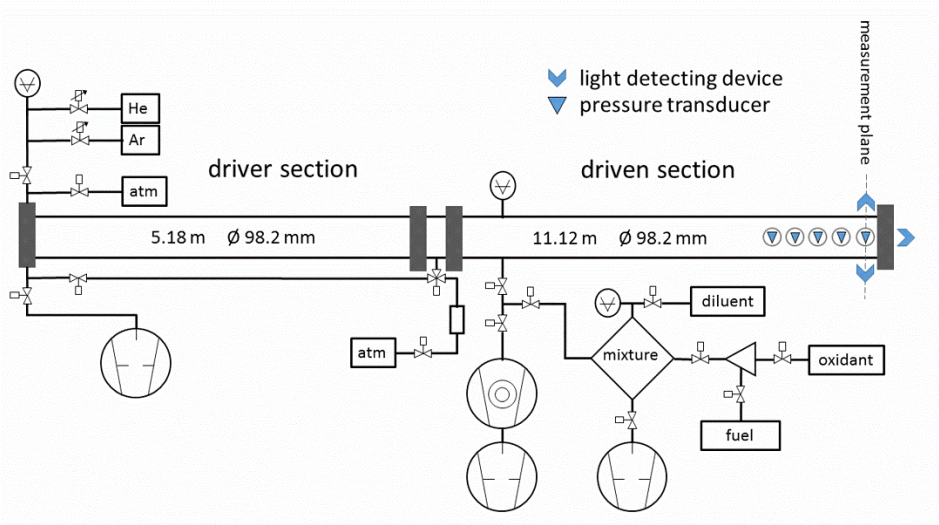

FIGURE 1: Schematic diagram of the shock tube [22, 25]. The measurement plane is located 10 mm from the end flange.

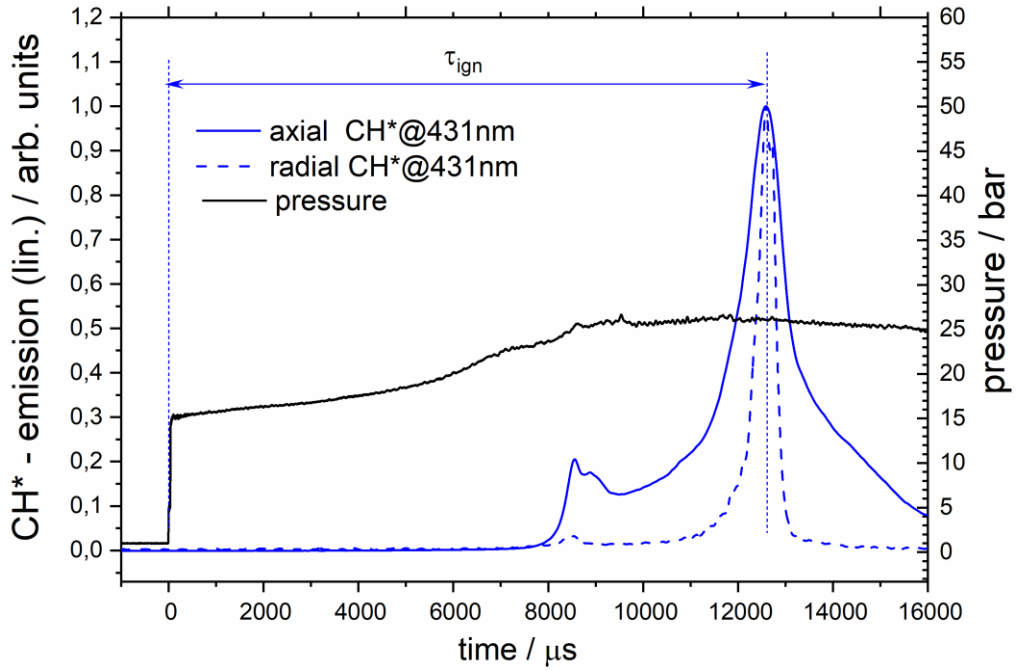

FIGURE 2: Example of pressure and emission signals of a typical OME_2 / synthetic air mixture with an extended observation period for: φ = 1.0, p_{init} = 14.4 bar, T_{init} = 868 K, and a dilution of 1:5 with N_2.

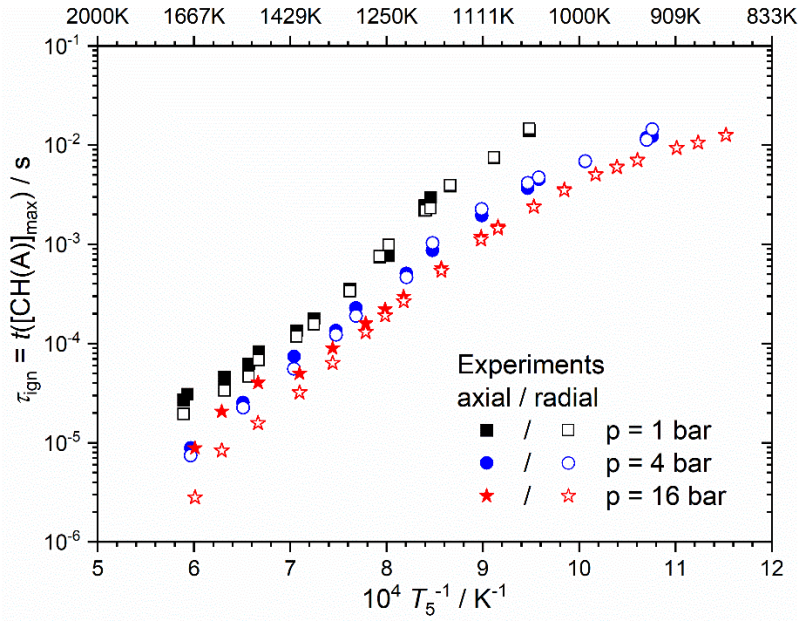

FIGURE 3: Ignition delay times (τ_{ign}) of OME_2 / synthetic air mixtures diluted 1:5 with N_2 at initial pressures p / bar = 1, 4, and 16.

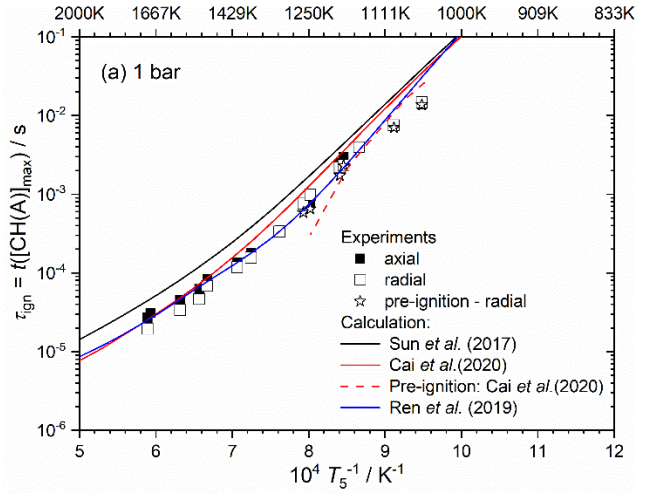

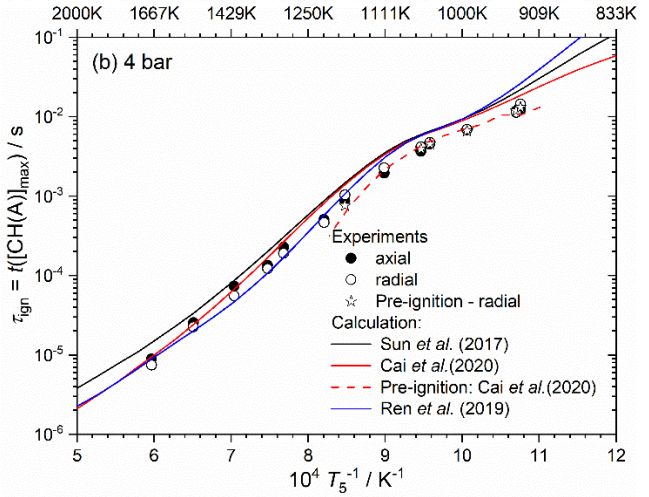

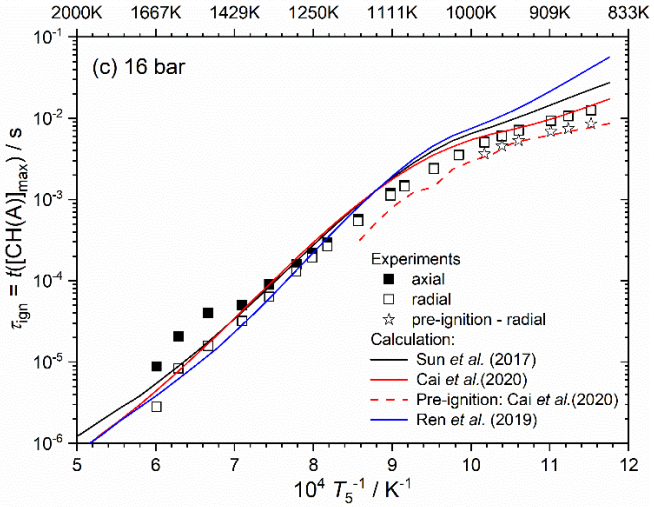

FIGURE 4: Comparison of measured (symbols) and simulated (curves) ignition delay times of stoichiometric OME_2 / synthetic air mixtures diluted 1:5 with N_2 for p / bar = 1, 4, and 16 using $p = p(t)$.

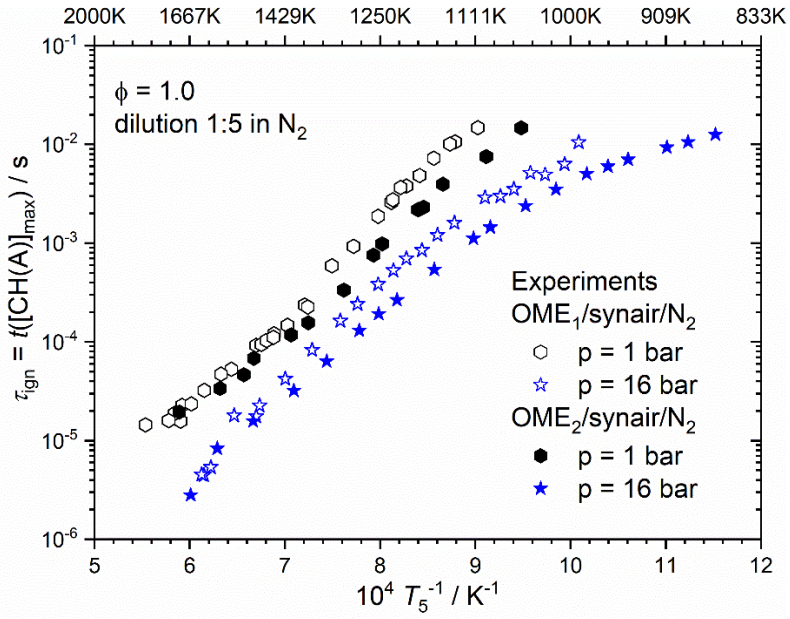

FIGURE 5: Comparison of measured ignition delay times (τ_{ign}) of synthetic air mixtures of OME_2 (*p.w.*) and of OME_1 [16], at initial pressures p / bar = 1 and 16, φ = 1.0 and 1:5 diluted with N_2. Only radially measured emission data shown.

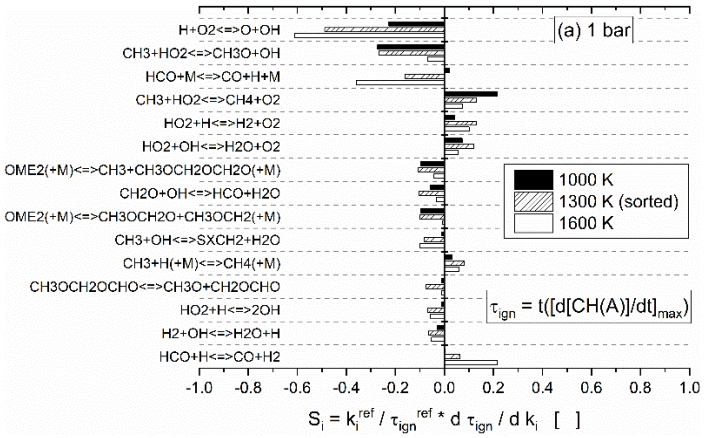

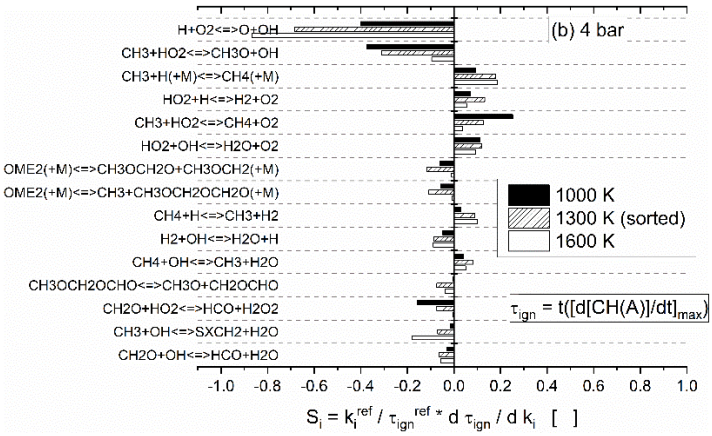

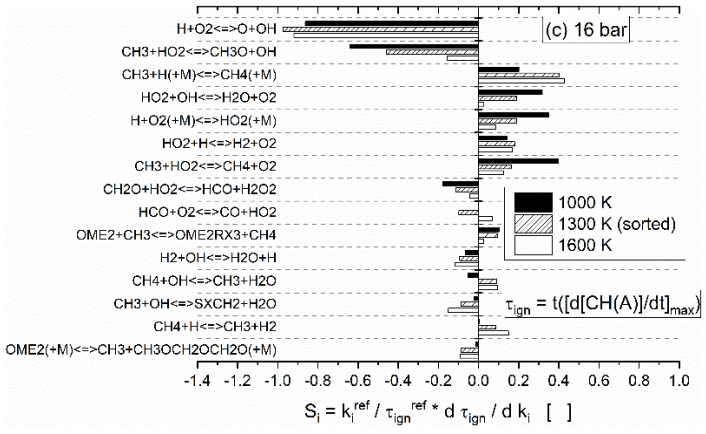

FIGURE 6: Sensitivity of ignition delay time for a mixture of OME_2 / synthetic air calculated for three different temperatures at p / bar = 1, 4, and 16, φ = 1.0, and a dilution d = 1:5 in N_2. Reaction model used: Cai *et al.* [14].

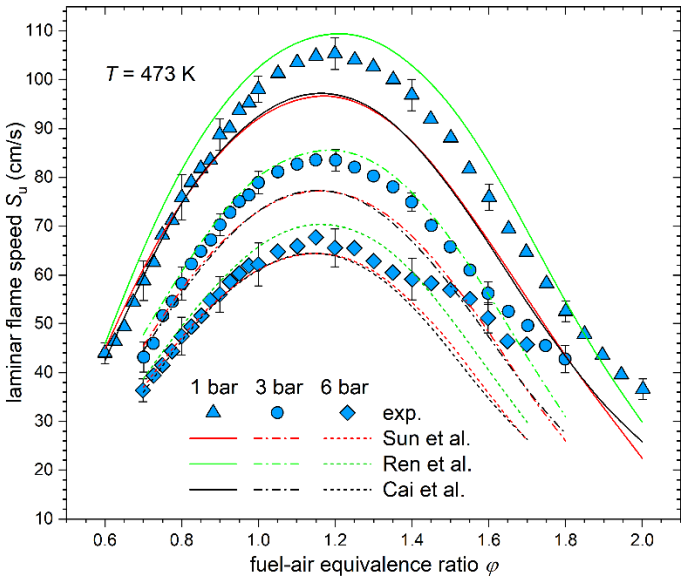

FIGURE 7: Measured laminar burning velocities of OME_2-air mixtures (symbols) and calculated laminar flame speeds (curves). Calculations using reaction models from Cai *et al.* [14], Sun *et al*. [20], and Ren *et al.* [21].

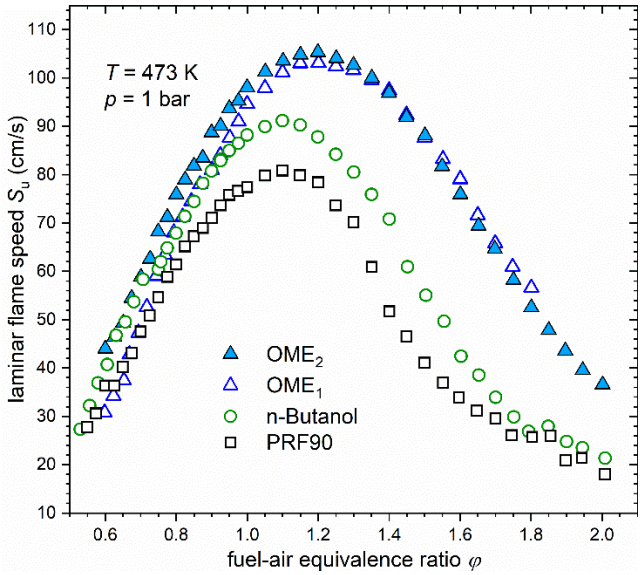

FIGURE 8: Comparison of the laminar burning velocities of OME_2-air mixtures to measurements of mixtures of OME_1-air [16], *n*-butanol-air [24], and PRF90-air [25] at p = 1 bar.

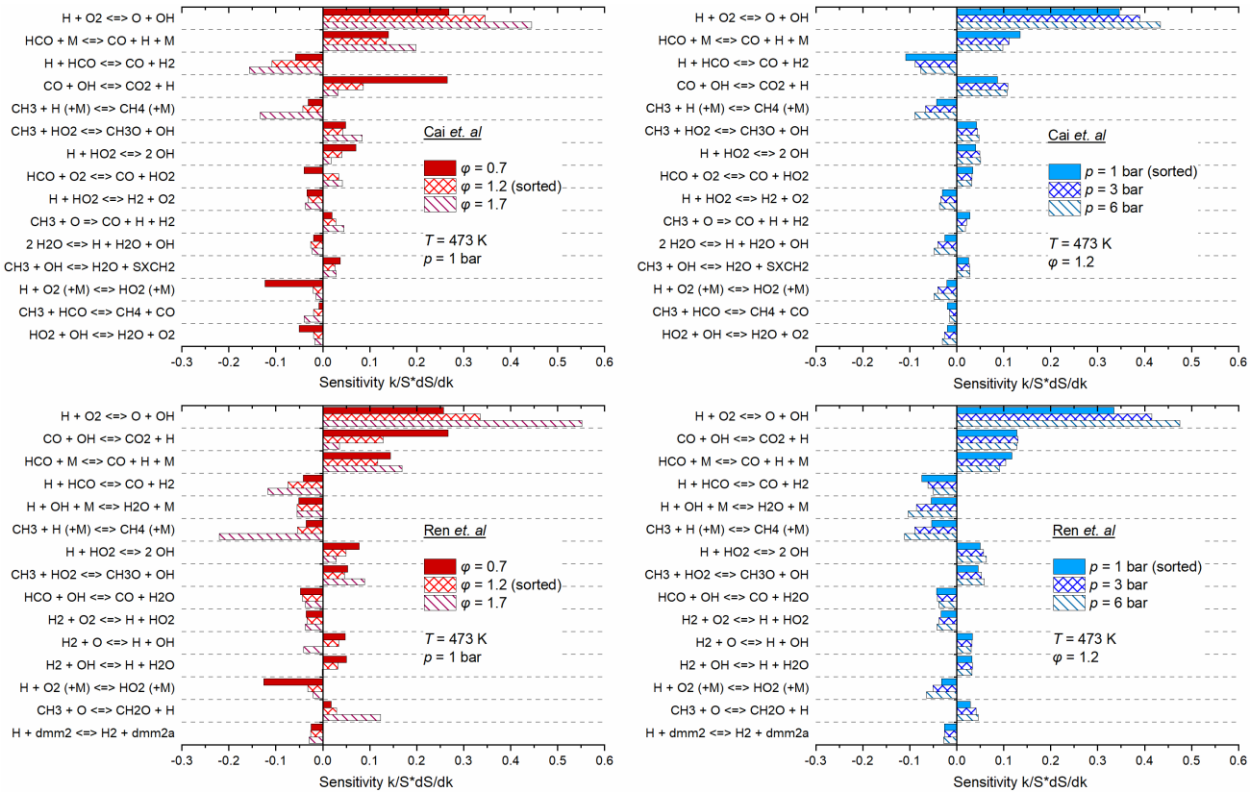

FIGURE 9: Sensitivity analyses of laminar flame speeds of OME_2-air mixtures as a function of φ at p = 1 bar (left) and of p at φ = 1.2 (right). Reaction models used: Cai *et al.* [14] (top) and Ren *et al*. [21] (bottom).